10

The Critical Feedback Level in Nanostructure-Based Semiconductor Lasers

F. Grillot [1][2], N. A. Naderi [2], M. Pochet [2], C.-Y. Lin [2] and L. F. Lester [2]
(1) Université Européenne de Bretagne, CNRS, Laboratoire Foton, INSA de Rennes, 20 Avenue des Buttes de Coësmes, 35708 Rennes, Cedex 7, France
(2) Center for High Technology Materials, The University of New Mexico, 1313 Goddard SE, Albuquerque, United States

1. Introduction

The extension of optical networks to local residential subscribers requires the development of extremely low-cost laser transmitter sources (Tohmori et al., 1997). While wafer fabrication allows for large-scale production, which drastically reduces the cost per laser, packaging remains a cost bottleneck, as it is not supported by parallel processing. Cost reduction must therefore be based on packaging simplification, such as flip-chip bonding and direct coupling of the laser into the fiber (Fernier et al., 1998). One of the characteristic problems of semiconductor lasers that complicates packaging is their sensitivity to external optical feedback. Fiber optic communication systems can be limited by unwanted optical feedback arising at fiber facets and junctions (Clarke, 1991), (Kitaoka et al., 1996). Although Faraday isolators are used extensively to reduce back reflections by as much as 60-dB, the elimination of the optical isolator remains a big challenge and is desirable because it leads to simplified packaging and will greatly reduce cost (Grillot et al., 2002). To understand the conditions under which the isolator can be eliminated, it is instructive to briefly review the physics of feedback in semiconductor lasers. This investigation naturally leads to highlighting the particular advantages of nanostructures in altering or improving the feedback resistance of the device.

The performance of a semiconductor laser can be strongly altered by external optical feedback. During early research, the importance of the distance between the laser facet and an external mirror reflector was pointed out in determining the nature of the semiconductor laser's response to optical feedback (Hirota & Suematsu, 1979). Even small reflections in the percent range were found to affect the laser stability dramatically. Although external optical feedback can be considered as a source of instability in many situations, it also can produce several beneficial effects that can improve laser performance. At the extremes of very weak and very strong optical feedback, linewidth narrowing and noise suppression can occur. This advantage, along with the large gain bandwidth of the semiconductor laser, can produce a highly tunable, narrow linewidth source that attracts many applications in spectroscopy, metrology and telecommunications (Kane & Shore, 2005).

Five distinct regimes based on spectral observation were reported for 1.55-μm distributed feedback (DFB) semiconductor lasers (Tkach & Chraplyvy, 1986). At the lowest feedback level, regime I, the laser operates on a single external cavity mode that emerges from the solitary laser mode. Depending on the phase of the feedback, the laser linewidth can be narrowed or broadened. Within regime II, the mode appears to split into two modes arising from rapid mode hopping. Noise-induced hopping between two external cavity modes is the underlying reason for this behavior. The transition to regime II has been shown to correspond to multiple solutions to the steady state equation that determines the frequency of the laser. This condition is satisfied when the parameter X_F is equal to unity in the following expression:

$$X_F = K_F \tau_e \sqrt{1+\alpha_H^2} \tag{1}$$

where τ_e is the external cavity roundtrip time while $K_F = (2C/\tau_i)\sqrt{R_p}$ is denoted as the feedback parameter. R_P is the feedback ratio and is defined as $R_P = P_1/P_0$ (with P_1 the power returned to the facet and P_0 the emitted power), C is the coupling coefficient from the laser facet to the external cavity, and τ_i is the internal roundtrip time within the laser cavity. The so-called linewidth enhancement factor (α_H-factor) corresponding to the coupling between the phase and the amplitude of the electric field is usually defined as follows:

$$\alpha_H = -\frac{4\pi}{\lambda}\frac{dn/dN}{dg/dN} = -\frac{4\pi\Gamma}{\lambda}\frac{dn/dN}{dG_{net}/dN} \tag{2}$$

where g is the material gain. The α_H-factor depends on the ratio of the evolution of the refractive index n with the carrier density N to that of the differential gain dg/dn. Γ is the optical confinement factor and $G_{net}=\Gamma g-\alpha_i$ is the net modal gain where α_i is the internal loss coefficient. The α_H-factor is used to distinguish the behavior of semiconductor lasers with respect to other types of lasers (Henry, 1982), and influences several fundamental aspects of semiconductor lasers, such as the linewidth (Su et al., 2004) and the laser behavior under optical feedback (Su et al., 2003). In regime III the laser re-stabilizes in a single external cavity mode (the lowest linewidth mode) with constant power. As the feedback level is further increased, the impact of optical feedback becomes independent of the external cavity length and the laser undergoes a transition to a chaotic state characterized by coherence collapse (CC) and denoted as regime IV (Lenstra et al., 1985). Coherence collapse or critical feedback is the common name given to describe the irregular dynamics occurring when the laser is operated above threshold, and has been greatly studied over the last twenty years. This regime has been described as co-existing chaotic attractors (Mork et al., 1988) and as an important source of noise (Mork et al., 1988), (Tromborg & Mork, 1990). The main consequence of the coherence collapse regime consists of a drastic collapse of the laser's coherence time leading to an enhancement of the laser's linewidth up to several gigahertz. For lasers used as an optical transmitter, the coherence collapse has been experimentally (Grillot et al., 2002) and theoretically (Clarke, 1991) demonstrated to cause a strong degradation in the bit error rate (BER). As the feedback level is further increased, the laser enters regime V, which is characterized by single-mode, constant intensity and narrow

linewidth operation. This regime can only be reached when laser diodes with antireflection coated facets are used.

The purpose of this chapter is to show both theoretically and experimentally that the variations of the above-threshold α_H-factor negatively impact the feedback level for which the coherence collapse regime occurs. The coherence collapse threshold is explored in nanostructure based semiconductor lasers, which in the context of this work encompasses quantum dot (QD), quantum dash (QDash), and quantum well (QW) structures. It is particularly well-known that QD and QDash based semiconductor lasers have attracted a lot of interest in the last decade owing to their expected remarkable properties arising from charge carrier confinement in the three space dimensions (Arakawa & Sakaki, 1982). Indeed, low threshold current densities and high material gain (Bimberg et al., 1997), (Liu et al., 1999), temperature insensitivity (Deppe et al., 2002), and reduced α_H-factor at the lasing wavelength (Saito et al., 2000), (Martinez et al., 2005) have been reported. This latter property combined with a high damping factor (O'Brien et al., 2003), (Erneux et al., 2008) was found to be of utmost importance because it should increase the tolerance to optical feedback in these devices (Azouigui et al., 2007), (Su et al., 2003) and may also offer potential advantages for direct modulation without transmission dispersion penalty.

However, in some cases, the above-threshold α_H-factor was experimentally found to be much larger as compared to traditional QW lasers ([a]Grillot et al., 2008), (Dagens et al., 2005). Such an enhancement is naturally not beneficial in practice for many reasons (Henry, 1982) and it provokes a rapid collapse of the laser's coherence time. Thus, considering the energy level contributions such as the ground state (GS) and the excited state (ES), this chapter shows that the analytical relation giving the onset of the critical feedback level can be rewritten. The carrier filling from the ES is found to produce an additional term, which accelerates the route to chaos. Also depending on how the above-threshold α_H-factor behaves, the critical feedback level can exhibit two different trends with output power. Thus, the influence of the ES coupled to the emphasized non-linear effects makes such devices more sensitive to optical feedback causing larger variations in the onset of the coherence collapse. These results highlight that the control of the α_H-factor has to be considered as a significant input for the realization of feedback-resistant lasers. It is also pointed out that the prediction of the onset of the coherence collapse remains an important feature for all applications requiring a low noise level or a proper control of the laser coherence.

2. Predicting the onset of the critical feedback regime

Different analytical models giving the onset of the coherence collapse have been derived over the last twenty years. This section aims to provide an overview of the most relevant relations estimating this critical feedback level.

2.1 Optical Power Transfer Function Analysis

This model was derived from the microwave modulation characteristics of laser diodes (Helms & Petermann, 1989). Starting from the conventional rate equations for a single-mode laser diode with optical feedback evaluated through small-signal analysis, it was shown that the modulation transfer function of a feedback laser can be expressed as:

$$H_K(j\omega_m) = (1 - K(j\omega_m)) \frac{H(j\omega_m)}{1 - K(j\omega_m) H(j\omega_m)} \tag{3}$$

where ω_m is the modulation frequency. In (3), $H(j\omega_m)$ is the normalized transfer function of the laser diode in the absence of optical feedback given by:

$$H(j\omega_m) = \frac{1}{\left(j\frac{\omega_m}{\omega_r}\right)^2 + \left(j\frac{\omega_m}{\omega_d}\right) + 1} \tag{4}$$

ω_r and ω_d are the relaxation and damping resonance frequencies, respectively. Equation (3) is derived for the minimum linewidth mode due to its high degree of stability over other cavity modes (Shunk & Petermann, 1988). The modification of the solitary laser modulation response due to weak feedback and α_H>1 is found to be (Helms & Petermann, 1989):

$$K(j\omega_m) = j\frac{K_F}{\omega_m}\sqrt{1+\alpha_H^2}\left(1 - e^{-j\omega_m \tau_e}\right) \tag{5}$$

Examination of (3) reveals that the system will be unstable due to a small perturbation if an unstable pole occurs. The existence of such a pole does not necessarily mean that coherence collapse occurs but the minimum feedback level at which an unstable pole occurs does correspond to the onset of the coherence collapse. As a result, considering the case of a long external cavity (e.g. $\omega_r \tau_e$>>1) as well as $\omega_m \approx \omega_r$ and $\omega_r << \omega_d$, the unstable pole occurs in (3) when $K(j\omega_m)H(j\omega_m)$=1. This condition leads to an analytical expression for the onset of coherence collapse expressed by:

$$R_{Pc} = \left(\gamma\frac{\tau_i}{4C}\right)^2 f(\alpha_H) \tag{6}$$

with $\gamma = \omega_r^2/\omega_d$ the damping factor in rad/sec and $f(\alpha_H) = 1/\left(1+\alpha_H^2\right)$. Expression (6) depends only on the solitary laser response and the α_H-factor. There is no explicit dependence on the external cavity length since a long-cavity asymptotic assumption was used in the derivation. For the case of a short external cavity (e.g. $\omega_r \tau_e$<<1), the onset of the coherence collapse is found to be dependent on the external cavity length as demonstrated in (Shunk & Petermann, 1989). In validating equation (6) against numerical simulations of an external cavity laser diode, it was shown that the expression deviated from the numerical results for low α_H-factor values. Consequently, the expression for the critical feedback level was found empirically driven by the same expression but instead $f(\alpha_H)$ is replaced by $g(\alpha_H)$, which is expressed as: $g(\alpha_H) = (1+\alpha_H^2)/\alpha_H^4$. This relation theoretically predicts that coherence collapse does not occur if $\alpha_H \to 0$, as explained through Henry and Kazarinov's ellipse whose eccentricity decreases with the α_H-factor (Henry & Kazarinov, 1986). For the case where α_H=0, all the fixed points describing the stability of the system (*modes* and *antimodes*) are located on a circle around the solitary laser mode. Under this condition, the

minimum gain mode and the minimum linewidth mode are the same and do not compete with each other and thereby coherence collapse cannot occur (Henry & Kazarinov, 1986). Despite a general agreement that the critical feedback level may be strongly up-shifted for low α_H-factors ([a]Grillot et al., 2008), the complete suppression of the critical feedback level has never been reported. This last condition has been particularly expected for QD and QDash lasers because of their remarkable properties arising from charge carrier confinement in three spatial dimensions (Arakawa & Sakaki, 1982) and lower α_H-factors (Bimberg et al., 1997), (Newell et al., 1999).

2.2 External Cavity Mode Analysis

Based on the Lang and Kobayashi rate equations (Lang & Kobayashi, 1980) in the presence of optical feedback, the variation of the angular frequency induced by external optical feedback can be written as:

$$\Delta\omega\tau_i = (\omega - \omega_0)\tau_i = -2C\sqrt{R_P}\sqrt{1+\alpha_H^2}\,\sin\left(\varphi + \tan^{-1}(\alpha_H)\right) \tag{7}$$

with φ the phase of the feedback wave and ω_0 the pulsation of the free-running laser. (Henry & Kazarinov, 1986) demonstrated that the onset of the coherence collapse occurs when the feedback parameter K_F, given in (1), is comparable to the relaxation frequency ω_r. Thus, based on (7), the onset of the coherence collapse can be determined when the frequency shift is maximized ($\Delta\omega_{\max}\tau_i = 2C\sqrt{R_{PC}}\sqrt{1+\alpha_H^2}$) for a certain critical feedback level. A strong increase in the optical power spectrum at $\omega_0 \pm \omega_r$ marks the feedback level defining the transition to the coherence collapse regime when $\Delta\omega_{\max} \geq \omega_r$. As a result, the onset of coherence collapse can be calculated via the following relationship (Binder & Cormarck, 1989):

$$R_{P_c} = \left(\omega_r \frac{\tau_i}{2C}\right)^2 f(\alpha_H) \tag{8}$$

Although this equation is based on a model considering only the steady-state solutions under optical feedback, it was shown to agree with predictions made in (Shunk & Petermann, 1988) and (Henry & Kazarinov, 1986). Compared with (6), this new expression does not include the damping rate, which has been found to be much larger in QD and QDash based devices compared to QW ones (O'Brien et al. 2003), ([b]Grillot et al., 2008).

Another expression similar to (8) but with $(2)^{1/2}$ instead of a 2 in the numerator was derived by analyzing the stability of the oscillation condition solutions for a laser under optical feedback (Mork et al., 1992). Coherence collapse is seen as a chaotic attractor and that chaos is reached for increasing feedback levels through a quasi-periodic route interrupted by frequency locking. For a long external cavity ($\omega_r\tau_e >> 1$), this new expression provides an approximation to the value of the feedback parameter K_F at which instability sets in.

Because the two approaches discussed in this section are highly similar, (8) can be rewritten as:

$$R_{P_C} = \left(\omega_r \frac{\tau_i}{pC} \right)^2 f(\alpha_H) \tag{9}$$

with p=2 or $(2)^{1/2}$ depending on the model under consideration.

2.3 Mode Competition Theory

The generation mechanism for excess intensity noise due to optical feedback has been analyzed theoretically and experimentally in (Yamada & Suhara, 1990). Modal rate equations under the weakly coupled condition with external optical feedback were derived which account for the mode competition phenomena found in Distributed Feedback (DFB) and Fabry-Perot (FP) lasers. The critical optical feedback level was calculated by confirming the build-up of external cavity modes and expressed as follows (Yamada & Suhura, 1990), (Suhura & Yamada, 1993):

$$R_{P_C} = 22R \left[\frac{nL}{l(1-R)} \right]^2 = \frac{11}{2C^2} \left(\frac{nL}{l} \right)^2 \tag{10}$$

with L and l the lengths of the laser cavity and the external cavity, respectively, n the refractive index and R the reflectivity of the emitting facet. The critical feedback level was found to be inversely proportional to the distance squared (l^2) to the reflection point. This relation, which holds only for FP lasers, was used to analyze the generation of the excess noise on the basis of mode competition theory and calculated the minimum noise level in the presence of external optical feedback. Calculations have shown that external cavity modes build up above a critical level of external optical feedback and result in excess noise due to the competition between external cavity modes and lasing modes. This method does not account for variations in the bias current, limiting its applicability for devices that have characteristic parameters that vary as the bias current is changed.

3. Recent advances in nanostructure-based semiconductor lasers

Low cost, directly modulated lasers will play a major role in the next generation telecommunication links (Local and Metropolitan Area Networks) for uncooled and isolator-free applications. Materials grown on an InP substrate have generally been the reference systems for 1.55-µm applications. Actual laser sources which are based on the InGaAsP/InP QW active material exhibit typical threshold currents lower than 10mA and a characteristic temperature T_0 of ~ 60 K (20-80 °C) (Thijs et al., 1994), (Phillips et al., 1999). More recently, GaInAlAs/InP QW lasers have shown an improved T_0 of ~ 90 K from 20 to 120 °C owing to a higher conduction band offset. Lasers realized in this material system allowed data transmission over a 40 km fiber span at 10Gbps up to 80°C (Stegmuller et al., 1993), (Makino et al., 2005). Temperature-insensitive lasers fabricated on GaAs are very attractive for low-cost high volume production due to a reduced cost of GaAs wafers and a mature technology. Two approaches have been intensively investigated in the last decade namely InAs QDs and GaInAsN QW emitting in the 1.3-µm window. GaInAsN(Sb) alloys grown on GaAs substrates extend the emission wavelength further into the 1.55-µm band.

This material system offers high electron confinement, a prerequisite for high T_0, and a high differential gain. A recent result of GaInAsNSb/GaAs QWs emitting at 1.55-µm shows a relatively low threshold current density of 579 A/cm² with propagation losses of ~ 4.8 cm^{-1} (Bank et al., 2006). However, due to a lower material gain, typical threshold currents of ridge waveguide lasers amount to 60mA (Gupta et al., 2006). The less mature material of GaInAsNSb development obviously needs further improvements. Many efforts have been devoted to the GaAs-based QD material system for emission in the 1.3-µm band, owing to a better material maturity (Bimberg et al., 1997), (Liu et al., 1999), (Deppe et al., 2002), (Saito et al., 2000), (Martinez et al., 2005), which allowed the demonstration of temperature insensitive 10Gbit/s transmission up to 85°C (Gerschütz et al., 2006), (Dagens et al., 2006). However for long-haul telecomm applications, lasers emission at 1.55-µm is mandatory. Two different approaches can match this application: metamorphic QDs grown on GaAs and QDs grown on InP substrates. Laser emission up to 1.45-µm has recently been demonstrated using metamorphic InAs/GaAs QD layer. The typical threshold current density equals ~ 1-1.5 kA/cm², and the characteristic temperature is ~65K (20-85 °C) (Karachinsky et al., 2005). More recently, coupled QD-QW tunnel injection lasers present a very low threshold current density of 63 A/cm² and an interesting 3-dB modulation bandwidth of ~ 8 GHz (Mi et al., 2006). But further extension of the emission wavelength at 1.55-µm on GaAs remains an issue. So far, only QD-based active layers grown on InP have allowed emission in the telecommunication window. Growth of QDs on (100) substrates has already been demonstrated using Molecular Beam Epitaxy (MBE) (Kim et al., 2004), or Molecular Organic Vapor Phase Epitaxy (MOVPE) (Franke et al., 2001). Elongated dots, or so-called QDashs have also been obtained by MBE (Wang et al., 2001), (Deubert et al., 2005) which have led to the demonstration of high performance lasers (Lelarge et al., 2007). An alternative approach is the use of the InP(311)B wafer orientation, which has also enabled demonstration of 3D confined nanostructures with a QD density as high as 10^{11} cm^{-2} (Caroff et al., 2005) with as well as low chirp of a 2.5Gbps directly-modulated single mode waveguide laser emitting at 1.6-µm (Saito et al., 2001). As an example, fig. 1 represents 1×1-µm² atomic force microscopy (AFM) images of QDs and QDashs grown on InP(311)B and InP(001) substrates, respectively. Let us note that very recently, dynamic properties of InAs/InP(311B) QD lasers emitting on the GS at 1.52-µm have been reported. The α_H-factor is found to be as low as 1.8 at the gain peak just below threshold and increases to about 7 above threshold but remains constant with the current. The rather high value is attributed to band filling of the thick wetting layer high degeneracy states. The sole emission from the GS at high current and at a high temperature of 75°C as well as a distinct relaxation oscillation peak in the frequency modulation response indicate the absence of phonon relaxation bottleneck originating from an ES (Martinez et al., 2008), ([c]Grillot et al., 2008).

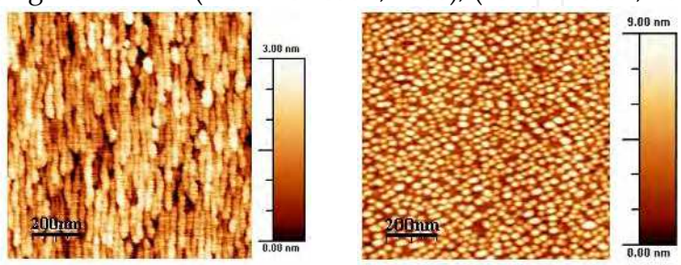

(a) (b)

Fig. 1. (a) 1x1-µm² Atomic Force Microscopy images of the InAs QDashs (a) and (b) QDs.

4. Results and discussion

This section gives the experimental results on both the static and the dynamic characteristics of the semiconductor lasers under study.

4.1 Device description

The device structure shown in fig. 2 was grown on an n^+-InP substrate. The active region is a dot-in-well (DWELL) structure consisting of 5 layers of InAs QDashs embedded in compressively-strained $Al_{0.20}Ga_{0.16}In_{0.64}As$ QWs which are separated by 30-nm un-doped tensile-strained $Al_{0.28}Ga_{0.22}In_{0.50}As$ spacers. Each side of the active region is surrounded by 105-nm waveguide layers of lattice-matched $Al_{0.30}Ga_{0.18}In_{0.52}As$. The p-cladding layer is step-doped AlInAs with a thickness of 1.5-μm to reduce free carrier loss and the n-cladding is a 500-nm thick layer of AlInAs. The laser structure is capped with a 100-nm InGaAs layer. Processing consisted of patterning a four-micron wide ridge waveguide with a 500-μm cleaved cavity length.

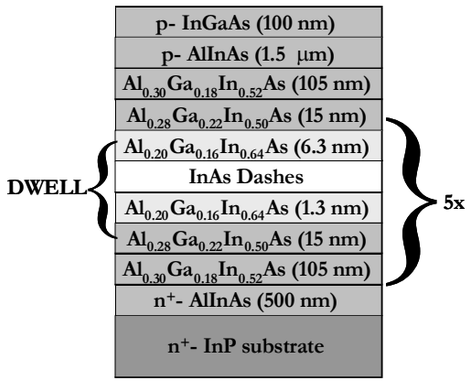

Fig. 2. Layer structure of the InAs/InP QDash Fabry-Perot (FP) device fabricated with the DWELL technology

The threshold current leading to a GS-emission is ~45mA and the external differential efficiency is about 0.2W/A. Beyond a pump current of ~100mA, ES lasing emission occurs. Fig. 3 shows the light-current characteristic measured at room temperature. As observed in fig. 3, the onset of ES lasing leads to a kink in the light-current characteristics as well as a modification of the slope efficiency (Veselinov et al., 2007)

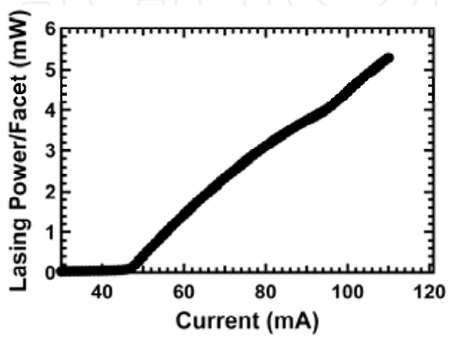

Fig. 3. The light current characteristic of the QDash FP laser under study

4.2 Effective gain compression

Conventional small-signal analysis of the semiconductor laser rate equations leads to a damped oscillator solution that is characterized by a relaxation frequency and an associated damping rate. To account for saturation of the optical gain generated by the semiconductor media with the photon density in the cavity, it is common to include a so-called gain compression term as well (Coldren & Corzine, 1995). Measuring the frequency response as a function of the output power is a common method to evaluate gain compression in semiconductor lasers. In the case of the QD laser, it has been shown that effects of gain compression are more important than those measured on QW devices (Su et al., 2005), (Su & Lester, 2005). In order to explain this phenomenon, a modified nonlinear gain coefficient has been introduced leading to a new expression for the relaxation frequency under strong gain saturation (Su & Lester, 2005):

$$f_r^2 = \frac{v_g a S}{4\pi^2 \tau_p (1+\varepsilon_S S)} \approx \frac{v_g a_0 S}{4\pi^2 \tau_p (1+\varepsilon_{Seff} S)} \tag{11}$$

with v_g being the group velocity, a the differential gain, a_0 the differential gain at threshold (unsaturated value), S the photon density, τ_p the photon lifetime, ε_S the gain compression factor related to the photon density and ε_{Seff} the effective gain compression factor which is defined as**:**

$$\varepsilon_{Seff} = \varepsilon_S \frac{1}{1-\frac{g_{th}}{g_{\max}}} \tag{12}$$

where g_{th} is the gain at threshold and g_{max} is the maximum gain for GS-lasing. Equation (12) indicates that the gain compression is enhanced due to gain saturation by a factor of $g_{max}/(g_{max}-g_{th})$. In Fig. 4 the evolution of the normalized gain compression $\varepsilon_{Seff}/\varepsilon_S$ is plotted as a function of the ratio g_{max}/g_{th}. This shows that the higher the ratio g_{max}/g_{th} the lower the effects of gain compression. If $g_{max} >> g_{th}$ the graph tends to an asymptote such that $\varepsilon_{Seff}/\varepsilon_S \rightarrow 1$. For cases where $g_{max} \rightarrow g_{th}$, gain compression effects are strengthened: the ratio increases drastically and can be extremely large if not enough gain is provided within the structure ($g_{max} \approx g_{th}$). As an example, for the QD laser under study, $g_{max}/g_{th} \approx 2$ meaning that the effects of gain compression are doubled causing critical degradation to the laser bandwidth.

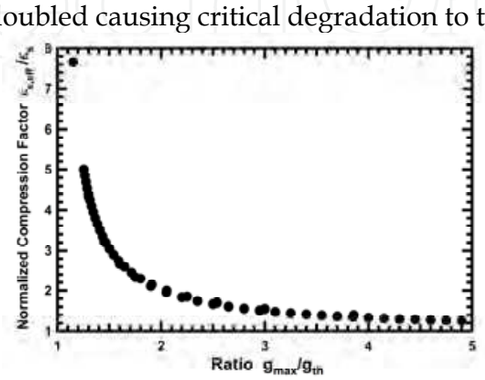

Fig. 4. Normalized compression factor as a function of g_{max}/g_{th}

Applying this same theory to the case of the QDash laser, the square of the measured resonance frequency is plotted in fig. 5 as a function of the output power, which is linked to the photon density through the relation $P = h\nu V v_g \alpha_m S$ with $h\nu$ the energy per photon, V the cavity volume and $\alpha_m v_g$ the energy loss through the mirrors, α_m being the mirror loss. The experimental dependence of the relaxation oscillation frequency shows a deviation from the expected proportionality given by expression (11) (case with $\varepsilon_S = 0$) on the square root of the optical output power. Thus, the experimental trend depicted in fig. 5 for the QDash laser is modelled via the following relation (Su & Lester, 2005):

$$f_r^2 = \frac{AP}{1+\frac{P}{P_{sat}}} = \frac{AP}{1+\varepsilon_P P} \tag{13}$$

The curve-fit based on equation (13) is used to express the gain compression in terms of a saturation power such that $\varepsilon_S S = \varepsilon_P P = P/P_{sat}$ with ε_P the gain compression coefficient related to the output power P. The value of P_{sat} is indicative of the level of output power where nonlinear effects start to be significant. For the QDash device under test, the curve-fit leads to a P_{sat} < 17mW and a gain compression coefficient of approximately $\varepsilon_P = 1/P_{sat} \approx 0.06$ mW^{-1}. The maximum of the resonance frequency can be directly deduced from the curve-fitting as $\Omega_r = (AP_{sat})^{1/2}$ and was expected to be ~7.6GHz. Taking into account the facet reflectivity as well as the modal volume of the laser, the order of magnitude for the gain compression factor ε_S is in the range of 5×10^{-15} cm^3 to 1×10^{-16}cm^3 which is much larger than the typical values measured on conventional QW lasers (typically around 10^{-17} cm^3) (Petermann, 1988).

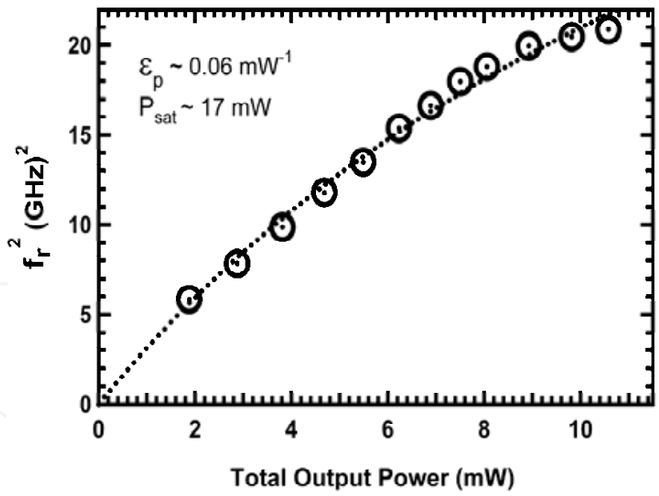

Fig. 5. The square of the resonance frequency versus the output power (open circles)

In fig. 6, the evolution of the damping rate against the relaxation frequency squared leads to a K-factor of 0.45ns as well as an effective carrier lifetime of γ_N^{-1}=0.16ns. The maximum intrinsic modulation bandwidth $f_{\max} = 2\pi\sqrt{2}/K$ is 19.7GHz. This f_{max} is never actually achieved in the QDash laser because of the aforementioned gain compression and the short effective carrier lifetime.

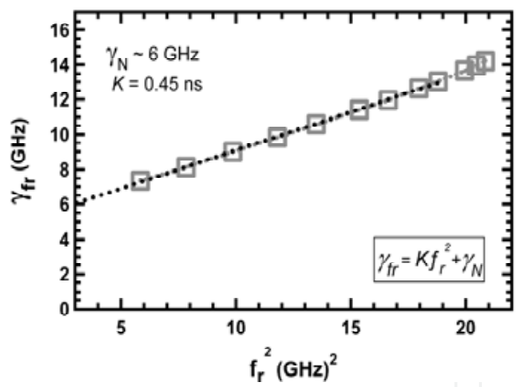

Fig. 6. The damping factor versus the square of the relaxation frequency

4.3 On the above-threshold α_H -factor

The above-threshold GS α_H-factor was measured using the injection locking (IL) technique, which is based on the asymmetry of the stable locking region over a range of detuning on both the positive and negative side of the locked mode (Liu et al., 2001). Using the IL technique, the α_H-factor can be determined using the following relationship:

$$\alpha_H = \sqrt{\left(\frac{\Delta\lambda_+}{\Delta\lambda_-}\right)^2 - 1} \tag{14}$$

where $\Delta\lambda = \Delta\lambda_{master} - \Delta\lambda_{slave}$, and $\Delta\lambda_{+/-}$ reflects the master's wavelength being either positively or negatively detuned with respect to the slave's wavelength. The ratio of $\Delta\lambda_+/\Delta\lambda_-$ should theoretically remain the same for any value of side mode suppression ratio (SMSR), which was kept at 35-dB for this measurement. The measured GS α_H-factor as a function of bias current is depicted in fig. 7. It was observed that the GS α_H-factor increased from ~1.0 to ~14 as the bias current was increased from the threshold value to 105mA. This enhancement is mostly attributed to the plasma effect as well as to the carrier filling of the non-lasing states (Wei & Chan, 2005), which results in a differential gain reduction above threshold. This strong degradation of the GS α_H-factor with the bias current produces a significant variation in the feedback sensitivity of the laser.

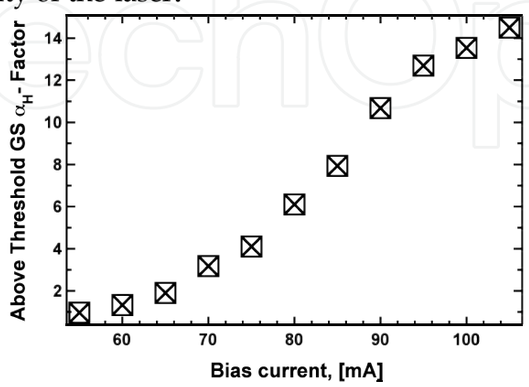

Fig. 7. The above threshold GS α_H-factor of the QDash laser versus the bias current measured by the injection-locking method.

On one hand, in QW lasers, which are made from a homogeneously broadened gain medium, the carrier density and distribution are clamped at threshold. As a result, the change of the α_H-factor is due to the decrease of the differential gain from gain compression and can be expressed as (Agrawal, 1990):

$$\alpha_H = \alpha_0(1+\varepsilon_P P) \tag{15}$$

where α_0 is the linewidth enhancement factor at threshold. Since the carrier distribution is clamped, α_0 itself does not change as the output power increases. As an example, fig. 8 shows the measured α_H-factor versus the output power for a 300-μm-long AR/HR coated DFB laser made from six compressively-strained QW layers. The threshold current is ~8mA at room temperature for the QW DFB device. Black squares correspond to experimental data. As described by equation (15), the effective αH-factor linearly increases with the output power to about 4.3 at 10mW. By curved-fitting the data in fig. 7, the α_H-factor at threshold is found to be around 4 while the gain compression coefficient equals ~$3x10^{-2}$ mW^{-1}. Compared to QD or QDash lasers, such a value of the gain compression coefficient is much smaller leading to a higher saturation power, which lowers the enhancement of the effective α_H-factor over the range of output power. It is worthwhile noting that modifying the laser's rate equations and including the effects of intraband relaxation, (15) can be reexpressed as follows (Agrawal, 1990):

$$\alpha_H = \alpha_0(1+\varepsilon_P P) + \beta\varepsilon_P P \frac{(1+\varepsilon_P P)}{(2+\varepsilon_P P)} \tag{16}$$

with β the parameter related to the slope of the linear gain which controls the nonlinear phase change. The situation for which β=0 corresponds to an oscillation purely located at the gain peak. For most cases, the second part of (16) usually remains small enough to be neglected.

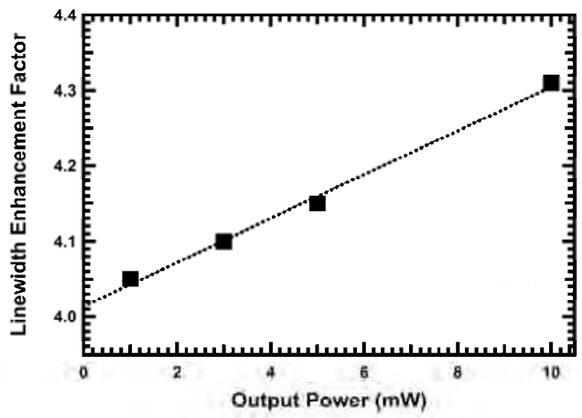

Fig. 8. The effective linewidth enhancement factor α_H as a function of the output power for the QW DFB laser.

On the other hand, in QD or QDash lasers, the carrier density and distribution are not clearly clamped at threshold. As a consequence of this fact, the lasing wavelength can switch

from GS to ES as the current injection increases meaning that a carrier accumulation occurs in the ES even though lasing in the GS is still occurring. The filling of the ES inevitably increases the α_H-factor of the GS and introduces an additional dependence with the injected current. Thus taking into account the gain variation at the GS and at the ES, the index change at the GS wavelength can be written as follows:

$$\delta n = \sum_{k=GS,ES} \alpha_k \delta g_k \tag{17}$$

with k being the index of summation for GS and ES respectively. Equation (2) leads to:

$$\delta n = \left(\alpha_{ES} \frac{a_{ES}}{a_{GS}} + \alpha_{GS} \right) \delta g_{GS} = \alpha_H \delta g \tag{18}$$

In equation (18), δg and δn are the changes of the gain and refractive index at the GS, respectively, αH is the linewidth enhancement factor actually measured in the device and evaluated at the GS-wavelength, a_{ES} and a_{GS} are the differential gain values at the ES and at the GS, respectively, α_{ES} describes the change of the GS index caused by the ES gain and α_{GS} is related to the GS index change caused by the GS gain variation. When the laser operates above threshold, α_{GS} keeps increasing with $\alpha_{GS}(1+\varepsilon_P P)$ as previously shown for the case of QW devices.

The gain saturation in a QD media can be described by the following equation (Su et al., 2005):

$$g_{GS} = g_{\max} \left[1 - e^{-\ln(2)\left(\frac{N}{Ntr} 1\right)} \right] \tag{19}$$

with N the carrier density and N_{tr} the transparency carrier density. When the laser operates above threshold, the differential gain for the GS lasing is defined as follows:

$$a_{GS} = \frac{dg_{GS}}{dN} = \frac{\ln(2)}{N_{tr}} \left(g_{\max} - g_{GS} \right) \tag{20}$$

with $g_{GS}=g_{th}(1+\varepsilon_P P)$ the uncompressed material gain increasing with the output power. Equation (19) leads to:

$$a_{GS} = a_0 \left(1 - \frac{g_{th}}{g_{\max} - g_{th}} \varepsilon_P P \right) = a_0 \left(1 - \frac{g_{th}}{g_{\max} - g_{th}} \varepsilon_S S \right) \tag{21}$$

with a_0 the differential gain at threshold. Then using equations (15), (18) and (21), the linewidth enhancement factor can be analytically written as:

$$\alpha_H(P) = \alpha_1\left(1+\varepsilon_P P\right) + \frac{\alpha_0}{1-\dfrac{g_{th}}{g_{\max}-g_{th}}\varepsilon_P P} \tag{22}$$

with $\alpha_1 \equiv \alpha_{GS}$ and $\alpha_0=\alpha_{ES}(a_{ES}/a_0)$. The first term in (22) denotes the gain compression effect at the GS (similar to QW lasers) while the second is the contribution of the carrier filling from the ES that is related to the gain saturation in the GS. For the case of strong gain saturation or lasing on the peak of the GS gain, equation (21) can be reduced to:

$$\alpha_H(P) = \frac{\alpha_0}{1-\dfrac{g_{th}}{g_{\max}-g_{th}}\varepsilon_P P} \tag{23}$$

In fig. 9, the normalized linewidth enhancement factor α_H/α_0 is calculated through equation (23) and represented in the (X,Y) plane with $X = P/P_{sat}$ and $Y = g_{max}/g_{th}$. This graph serves as a stability map and simply shows that a larger maximum gain is absolutely required for a lower and stable α_H/α_0 ratio. For instance let us consider the situation for which $g_{max}= 3g_{th}$: at low output powers i.e, $P < P_{sat}$, the normalized α_H-factor remains constant ($\alpha_H/\alpha_0 \sim 3$) since the gain compression is negligible. As the output power approaches and goes beyond P_{sat}, the ratio α_H/α_0 is increased. Gain compression effects lead to an enhancement of the normalized α_H-factor, which can go up to 10 for $P \approx 2P_{sat}$ level of injection for which the ES occurs.

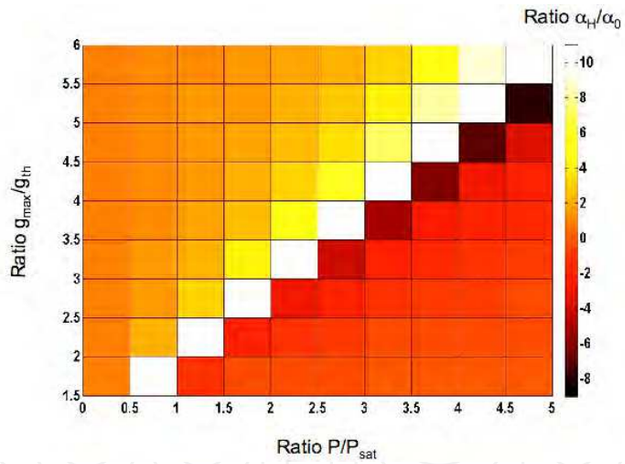

Fig. 9. Stability map based for the normalized linewidth enhancement factor α_H/α_0 in the (P/P_{sat}, g_{max}/g_{th}) plane.

Assuming that $g_{max} = 5g_{th}$, fig. 9 shows that the effects of gain compression are significantly attenuated since the ratio α_H/α_0 remains relatively constant over a wider range of output power. The level at which gain compression starts being critical is now shifted to $P \approx 3P_{sat}$ instead of $P \approx P_{sat}$. It is also important to note that at a certain level of injection, the normalized GS α_H-factor can even become negative. This effect has been experimentally reported in (Dagens et al., 2005) and occurs when the GS gain collapses, e.g when ES lasing occurs.

In fig. 10, the calculated GS α_H-factor (black dots) of the QD-laser from (Dagens et al., 2005) is depicted as a function of the bias current. Red stars superimposed correspond to data measurements from (Dagens et al., 2005) which have been obtained via the AM/FM technique. This method consists of an interferometric method in which the output optical signal from the laser operated under small-signal direct modulation is filtered in a 0.2nm resolution monochromator and sent in a tunable Mach-Zehnder interferometer. From separate measurements on opposite slopes of the interferometer transfer function, phase and amplitude deviations are extracted against the modulating frequency, in the 50MHz to 20GHz range (Sorin et al., 1992). The α_H-factor is given by the phase to amplitude response ratio at the highest frequency within the limits of the device modulation bandwidth. Fig. 10 shows a qualitative agreement between the calculated values and the values experimentally obtained. As expected, the GS α_H-factor increases with the injected current due to the filling of the excited states as well as carrier filling of the non-lasing states (higher lying energy levels such as the wetting layer). Although the α_H-factor is lowered at lower output powers, its increase with bias current stays relatively limited as long as the bias current remains lower than 150mA, e.g. such that $P<P_{sat}$. Beyond P_{sat}, compression effects become significant, and the α_H-factor reaches a maximum of 57 at 200mA before collapsing to negative values. As previously mentioned, the collapse in the α_H-factor is attributed to the occurrence of the ES as well as to the complete filling of the available GS states. In other words, as the ES stimulated emission requires more carriers, it affects the carrier density in the GS, which is significantly reduced. As a result, the GS α_H-factor variations from 57 down to -30 may be explained through a modification of the carrier dynamics such as the carrier transport time including the capture into the GS. This last parameter affects the modulation properties of high-speed lasers via a modification of the differential gain. These results are of significant importance because they show that the α_H-factor can be controlled by properly choosing the ratio g_{max}/g_{th}: the lower g_{th}, the higher g_{max}, and the smaller the linewidth enhancement factor. A high maximum gain can be obtained by optimizing the number of QD layers in the laser structure while gain at threshold is directly linked to the internal and mirror losses. Both g_{th} and g_{max} should be considered simultaneously so as to properly design a laser with a high differential gain and limited gain compression effects. The g_{max}/g_{th} ratio is definitely the key-point in order to obtain a lower α_H-factor for direct modulation in QD and QDash lasers.

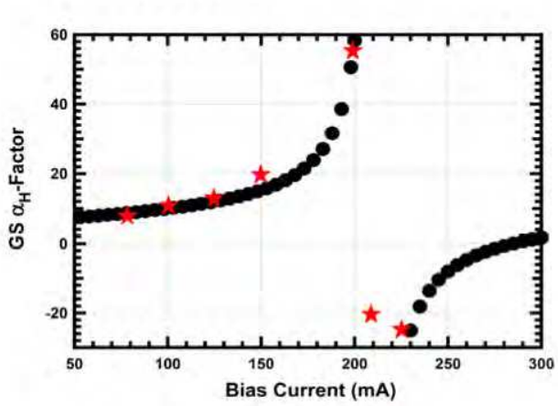

Fig. 10. Calculated GS α_H-factor for a QD laser versus the bias current (black dots). Superimposed red stars correspond to experimental data from (Dagens et al., 2005)

5. Optical feedback sensitivity

This sections aims to investigate the laser's feedback sensitivity by using different analytical models. Also the impact of the α_H-factor on the feedback degradation is carefully studied.

5.1 Description of the optical feedback loop

The experimental apparatus to measure the coherence collapse threshold is depicted in fig. 11. The setup core consists of a 50/50 4-port optical fiber coupler. Emitted light is injected into port 1 using a single-mode lensed fiber in order to avoid excess uncontrolled feedback. The optical feedback is generated using a high-reflectivity dielectric-coated fiber (> 95%) located at port 2. The feedback level is controlled via a variable attenuator and its value is determined by measuring the optical power at port 4 (back reflection monitoring). The effect of the optical feedback is analyzed at port 3 via a 10pm resolution optical spectrum analyzer (OSA). A polarization controller is used to make the feedback beam's polarization identical to that of the emitted wave in order to maximize the feedback effects. The roundtrip time between the laser and the external reflector is ~30ns. As a consequence, the long external cavity condition mentioned in the previous section $\omega_r \tau_e >> 1$ is fulfilled.

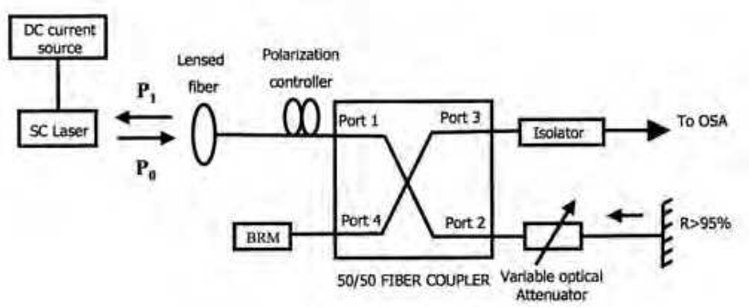

Fig. 11. Schematic diagram of the experimental apparatus for the feedback measurements

The long external cavity condition means that the coherence collapse regime does not depend on the feedback phase nor the external cavity length. Thus, in order to improve the accuracy of the measurements at low output powers, an erbium-doped-fibre-amplifier (EDFA) was used with a narrow band filter to eliminate the noise. The EDFA is positioned between the laser facet and the polarization controller (not shown in fig. 11). As already stated in section 1, the amount of injected feedback into the laser is defined as the ratio $R_{PdB} = 10\log(P_1/P_0)$ where P_1 is the power returned to the facet and P_0 the emitted one. The amount of reflected light that effectively returns into the laser can then be expressed as follows (Su et al., 2003):

$$R_{P\,dB} = P_{BRM} - P_0 + C \tag{24}$$

where P_{BRM} is the optical power measured at port 4, C is the optical coupling loss of the device to the fiber which was estimated to be about -4dB and kept constant during the entire experiment. The device is epoxy-mounted on a heat sink and the temperature is controlled at 20^0C. The onset of the coherence collapse was determined by monitoring the laser spectra

and noting when the linewidth begins to significantly broaden as shown in (Grillot et al., 2002), (Tkach & Chraplyvy, 1986). As an example, fig. 12 shows the measured optical spectra of a 1.5-μm QD DFB laser. The spectral broadening caused by the optical feedback at coherence collapse level, can significantly degrades the capacity of the high-speed communication systems.

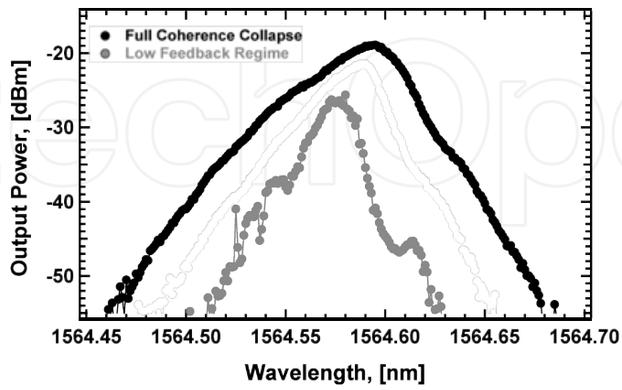

Fig. 12. Optical spectra of a 1.5-μm QD DFB laser. The solid black line corresponds to the fully developed coherence collapse

5.2 Evaluation of the critical feedback level

Based on (6) & (9), a strong degradation of the a_H-factor with the bias current should produce a significant variation in the laser's feedback sensitivity. In fig. 13, the measured onset of the coherence collapse is shown (black squares) for the QDash FP laser depicted in fig. 2 as a function of the bias current at room temperature Note that the dashed line in fig. 13 is added for visual help only. The feedback sensitivity of the laser is found to vary by ~20-dB over the range of examined current levels as the α_H-factor increases at higher bias currents. In order to compare the experimental data with theoretical models previously described, the onset of coherence collapse is calculated by substituting the measured relaxation frequency, damping factor and α_H-factor values directly into (6) and (9). Assuming a laser with cleaved facets, the coupling coefficient from the facet to the external cavity $C = (1-R)/2\sqrt{R}$ is calculated to be 0.6 and the internal round trip time in the laser cavity is about ~10ps. As shown in fig. 13, the best agreement with experimental data over the range of current is found with (9) for both values of p. The discrepancy between (9) is 3-dB which corresponds to the factor 2 as described in section 2.3. Such a difference remains within the experimental resolution of +/- 3-dB (see error bars in fig. 13). Using (6) leads to a larger discrepancy, whose minimum value is ~11-dB at 65mA. It is worth noting that for α_H–factors approaching unity (below 60mA), the critical feedback level saturates for all four models considered. This saturation is generated by the function $f(\alpha_H)$, which converges to 1 as α_H gets smaller. Experimentally, the trend does not saturate at this level of bias current since the resistance to optical feedback keeps increasing, demonstrating that the critical feedback level can be up-shifted for lower α_H–factors (Cohen & Lenstra, 1991).

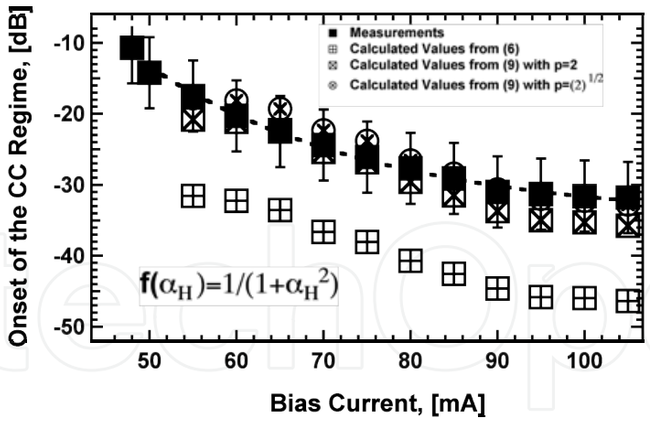

Fig. 13. Coherence collapse threshold as a function of the bias current for the QDash FP laser under study. Dashed line is added for visual help only.

In order to account for the α_H-factor approaching unity, the empirical function $g(\alpha_H)$ described in section 2.1 has been included in (6), and the results are depicted in fig. 14. Note that the dashed and solid lines in fig. 14 are added for visual help only. The calculated critical feedback level is now up-shifted for the lower values of the α_H-factor. At low bias currents, the measured values are found to be in a better agreement with calculations. Although (6) does not match the quantitative values in fig. 14, it qualitatively reproduces the up-shifting observed for small α_H-factors. This effect can be explained through variation of the α_H-factor, which changes $g(\alpha_H)$ by a factor of 500. Thus, at low bias currents, the feedback sensitivity is mostly driven by the $g(\alpha_H)$ function and not variations in the damping factor. Despite the fact that (6) was derived empirically under the assumption of weak optical feedback similar to a more complete analysis based on the Lang and Kobayashi phase equation (Alsing et al., 1996), (Erneux et al., 1996), it is found to exhibit a better accuracy for ultra-low α_H-factors. Thus, the discrepancy between the experimental data and theoretical prediction is decreased from 14-dB to 7-dB at 55mA. When extrapolating the dotted line in fig. 14 to 45mA, the calculated values will be very close to the experimental data. According to the mode competition based method given by expression (10), a critical feedback level of 58-dB is calculated using an external cavity length of 5m. This value is lower than the minimum value calculated with (6), which is about 45-dB. This feedback level corresponds to a critical level at which the external cavity modes start building-up but do not really correspond to the full coherence collapse regime.

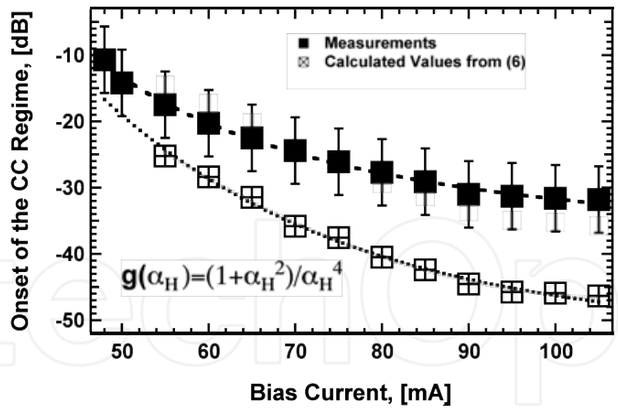

Fig. 14. Coherence collapse threshold as a function of the bias current for the QDash FP laser under study. Dashed and dotted lines are added for visual help only.

Fig. 15 shows the measured coherence collapse threshold as a function of the bias current for the QW laser studied in section 4.3. An increase in the critical feedback level is found to range between 36-dB to 27-dB when the current increases from 12mA to 70mA. In that situation, the onset of the coherence collapse follows a conventional trend (Azouigui et al, 2007), (Azouigui et al, 2009) driven by variations of the relaxation frequency.

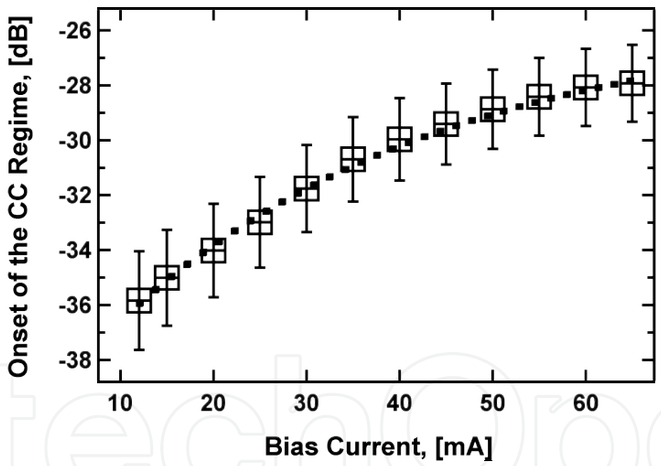

Fig. 15. Coherence collapse threshold as a function of the bias current for the QW DFB laser. The dotted line was added for visual help only.

5.3 Role of the ES in the feedback degradation

In QD or QDash lasers, it has been shown in section 4.3 that the α*H*-factor evaluated at the GS wavlength can be written as:

$$\alpha_H(P) = \alpha_{GS}(P, P_{sat}) + \alpha_{ES}(P, P_{sat}) \tag{25}$$

In (24), the first term denotes the gain compression effect at the GS while the second term represents the contribution of the carrier filling from the ES In the presence of a strong gain compression or when the second term in (25) dominates, the α_H-factor follows a non-linear trend above the laser threshold as previously shown. Based on the Lang and Kobayashi rate equations in the presence of optical feedback, it has been shown that an accurate way to calculate the onset of the coherence collapse regime is given by (9). Considering also expression (25), the mutual contributions of the GS and the ES can be considered together so as to re-write the critical feedback level for a QDash laser as follows:

$$R_{P_c}(dB) = R_{P_{c0}}(dB) + 10\log\left(\frac{1}{1+\dfrac{\alpha_{ES}(P,P_{sat})\left[\alpha_{ES}(P,P_{sat})+2\alpha_{GS}(P,P_{sat})\right]}{1+\alpha_{GS}^2(P,P_{sat})}}\right) \tag{26}$$

with,

$$R_{Pc0} = \left(2\pi f_r \frac{\tau_i}{pC}\right)^2 \frac{1}{1+\alpha_{GS}^2(P,P_{sat})} \tag{27}$$

The amount R_{Pc0} denotes the contribution of the GS only towards the change in the onset of the coherence collapse. The second term in (25) needs to be considered when the above threshold α_H-factor is dependant on contributions from both the GS (α_{GS}) and the ES (α_{ES}). Expression (26) goes a step further in the analytical description of the onset of the critical feedback level since it includes the additional dependence related to the ES itself.

Fig. 16 shows the calculated GS and ES contributions to the onset of the coherence collapse (with $p=2^{1/2}$) as a function of the bias current for the QDash FP laser depicted in fig. 4. In the calculations, an internal roundtrip time of 10ps and a coupling coefficient $C=(1-R)/2\sqrt{R}$ ~0.6 (for an as-cleaved laser) is considered. The saturation power P_{sat} is close to 17mW, the ratio g_{max}/g_{th} is about 1.5 while coefficients α_0 and α_1 are treated as fitting parameters and are such that $\alpha_0 << 1$ and $\alpha_1 \sim 2$. Solid lines in fig. 16 are used for guiding the eyes only. On one hand, when plotting only the contribution related to the gain compression at the GS (labeled [1]) given by (26), the critical feedback level is found to increase with the bias current As the laser's relaxation frequency is power dependent, such a variation is naturally expected. On the other hand, when considering only the contribution taking into account the carrier filling from the ES (labeled [2]) in (25), an opposite trend is observed. This contribution can be seen as a significant perturbation that results in a shift in the overall coherence collapse threshold. Thus, when both the GS and ES contributions are considered in the overall coherence collapse threshold, the calculated coherence collapse threshold is found to decrease with bias current (black solid line). Let us emphasize that these calculated values are in a good agreement with experimental data (black squares) except at low bias current for which a saturation is theoretically predicted around 23-dB. This discrepancy can be attributed to the fact that the amplitude of the optical feedback gets too large and does not match the low feedback assumption. As a conclusion, the overall

experimental trend depicted in fig. 16 appears unconventional since it does not match the relaxation frequency variations even at low bias current levels for which the coherence collapse is up-shifted. This different behavior is specific to QDash structures in which the non-linear effects associated with the ES can be much more emphasized. This phenomenon can make nano-structured lasers more sensitive to optical feedback, which results in larger variations in the onset of the coherence collapse compared to that of the QW devices.

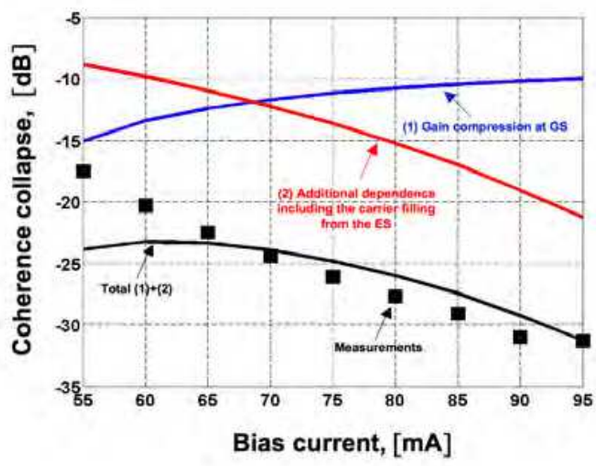

Fig. 16. Coherence collapse threshold as a function of the bias current including the contributions of the GS only, the ES only, both the GS and the ES and comparison with the measured data (black squares).

Fig. 17 shows the measured coherence collapse thresholds as a function of the α_H-factor for both the QDash FP laser (circles) and the QW DFB (squares). This figure illustrates how the route to chaos may change in a semiconductor laser; indeed depending on how the above-threshold α_H-factor behaves, the sensitivity to the coherence collapse may be improved or degraded. In regards to the QW device, the sensitivity to optical feedback is improved when increasing the current. This behavior, which has previously been observed (Azouigui et al., 2007), (Azouigui et al., 2009) is attributed to α_H-factor variations directly related to the relaxation frequency. Thus, the α_H-factor increases quite linearly above the laser's threshold and it remains mostly driven by the gain compression at the GS through the first term of equation (25) such that $\alpha_{GS} >> \alpha_{ES}$. Regarding the QDash device, the result shows a different situation: the resistance to optical feedback is substantially degraded with increasing bias current. This is due to the fact that the α_H-factor variations in the QDash FP laser are much more emphasized since for instance $\alpha_{GS} < \alpha_{ES}$ meaning that the carrier filling from the ES needs to be considered in order to explain the non-linear increase of the GS abovethreshold αH-factor. As a consequence, the critical feedback level does not follow the relaxation frequency variations since the coherence collapse is found to be up-shifted when decreasing the bias current level. Such behaviors can mostly occur in nano-structured lasers in which the influence of the ES coupled to the non-linear effects are emphasized. This phenomenon makes QD and QDash lasers more sensitive to optical feedback, thus the feedback

sensitivity can be very different from a laser to another, which results in larger variations in the onset of the coherence collapse as compared to QW devices. At the wavelength of 1.5-μm, the best feedback sensitivity was found to be 24-dB for a 205-μm Cleaved/HR QD DFB laser (Azouigui et al., 2007). This result can be explained by the combination of the cleaved facet that lowers the feedback sensitivity, a higher bias current (> 100mA) as well as smaller α_H-factor (α_H~4.5). For 1.3-μm wavelength range, higher tolerances to optical feedback have been reported in QD lasers with coherence collapse thresholds as high as 14-dB (Su et al., 2004) and 8-dB (O'Brien et al., 2003). Let us stress that making such a comparison with a QW FP laser instead of a QW DFB would not change the conclusion since on QW based structures the increase of the α_H-factor with current is limited as compared to QDash devices.

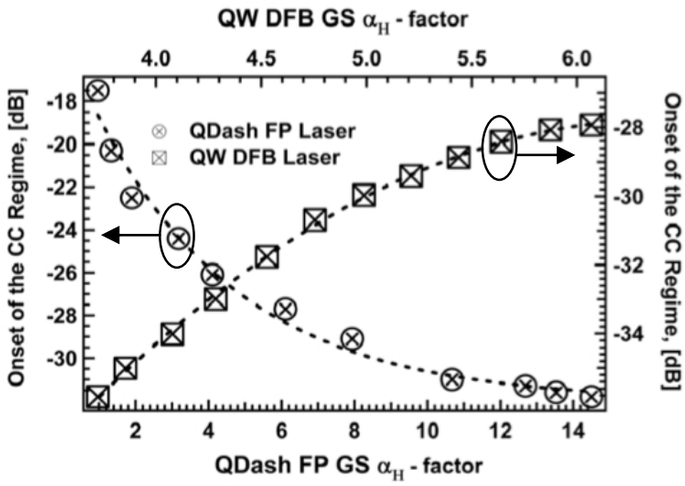

Fig. 17. Coherence collapse thresholds as a function of the α_H-factor for the QW laser (square markers) and for the QDash FP laser (circular markers) under study. Dashed lines are added for visual help.

6. Conclusions

The onset of the coherence collapse regime has been investigated experimentally and theoretically in 1.5-μm nanostructured semiconductor lasers. The prediction of the critical feedback regime has been conducted through different analytical models. Models based on the laser transfer function and on the mode competition analysis have been found to underestimate the onset of the critical feedback level. The models based on external cavity mode stability analysis have been found to be in good agreement with the experimental data. Although the model based on the transfer function has been widely used in the field of optical feedback, it does not systematically yield a strong agreement for nanostructure-based semiconductor devices except for the cases where an ultra low α_H-factor is considered. For QDash lasers, calculations are in agreement with the experiments that demonstrate that the ES filling produces an additional term, which accelerates the route to chaos. This contribution can be seen as a perturbation that reduces the overall coherence collapse threshold. Depending on the variations of the α_H-factor above threshold, the feedback

resistance can be improved or deteriorated from one laser to another. The design of QDash lasers with no ES, reduced gain compression effects, and a lower, quasi-constant α_H-factor remains a big challenge. Recently a promising result was achieved using a 1.5-μm InAs/InP(311B) semiconductor laser with truly 3D-confined quantum dots (Martinez et al., 2008) (cGrillot et al., 2008). The laser characteristics exhibited a relatively constant α_H-factor as well as no significant ES emission over a wide range of current. These results highlight that the control of the α_H-factor has to be considered as a significant input for the realization of feedback-resistant lasers. Also, the prediction of the onset of the coherence collapse remains an important feature for all applications requiring a low noise level or a proper control of the laser's coherence.

7. References

Agrawal, G. P., Effect of Gain and Index Nonlinearities on Single-Mode dynamics in Semiconductor Lasers, *IEEE J. Quantum Electron*., Vol. 26, 11, 1901-1909, 1990.

Alsing, P.M.; Kovanis, V.; Gavrielides, A. & Erneux, T., Lang and Kobayashi phase equation, *Phys. Rev. A*, Vol. 53, 4429-4434, 1996.

Arakawa, Y. & Sakaki, H., Multidimensional quantum well laser and temperature dependence of its threshold current, *Appl. Phys. Lett*., Vol. 40, 939-941, 1982.

Azouigui, S.; Dagens, B.; Lelarge, F.; Provost, J.G.; Accard, A.; Grillot, F.; Martinez, A.; Zou, Q. & Ramdane, A., Tolerance to Optical Feedback of 10Gbps Quantum-Dash based Lasers emitting at 1.55-μm, *IEEE Photon. Technol. Lett*, Vol. 19, 15, pp. 1181-1183, 2007.

Azouigui, S.; Dagens, B.; Lelarge, F.; Provost, J.-G.; Make, D.; Le Gouezigou, O.; Accard, A.; Martinez, A.; Merghem, K.; Grillot, F.; Dehaese, O.; Piron, R.; Loualiche, S.; Q. Zou and Ramdane, A., Optical Feedback Tolerance of Quantum-Dotand Quantum-Dash-Based Semiconductor Lasers Operating at 1.55 μm, IEEE J. of Select. Topics in Quantum Electron., Vol. 15, 764-773, 2009.

Bank, S.R.; Bae, H.P.; Yuen, H.B.; Wistey, M.A.; Goddard, L.L. & Harris, J.S., Jr., Room-temperature continuous-wave 1.55-μm GaInNAsSb laser on GaAs, *Electron. Lett*., Vol. 42, 156-157, 2006.

Bimberg, D.; Kirstaedter, N.; Ledentsov, N.N.; Alferov, Zh.I.; Kop'ev, P.S. & Ustinov, V.M., InGaAs-GaAs quantum-dot lasers, *IEEE J. of Select. Topics in Quantum Electron*., Vol. 3, 196-205, 1997.

Binder, J.O. & Cormarck, G.D., Mode selection and stability of a semiconductor laser with weak optical feedback, *IEEE J. Quantum Electron*., Vol. 25, 11, 2255-2259, 1989.

Caroff, P.; Paranthoën, C.; Platz, C.; Dehaese, O.; Bertru, N.; Folliot, H.; Labbé, C.; Piron, R.; Homeyer, E.; Le Corre, A.; & Loualiche, S., High-gain and low-threshold InAs quantum-dot lasers on InP, *Appl. Phys. Lett*, Vol. 87, 243107, 2005.

Clarke, R.B., The effects of reflections on the system performance of intensity modulated laser diodes", *J. Lightwave. Tech*, 9, 741-749, 1991.

Cohen, J.S. & Lenstra, D., The Critical Amount of Optical Feedback for Coherence Collapse in Semiconductor Lasers, *IEEE J. Quantum Electron*., Vol. 27, 10-12, 1991.

Coldren, L.A. & Corzine, S.W., Diode Lasers and Photonic Integrated Circuits, John Wiley & Sons, Inc., New York, 1995.

Dagens, B.; Markus, A; Chen, J. X.; Provost, J.-G.; Make, D.; Le Gouezigou, O.; Landreau, J.; Fiore, A. & Thedrez, B., Giant linewidth enhancement factor and purely frequency modulated emission from quantum dot laser, Vol. 41, 6, 323-324, 2005.

Dagens, B.; Bertran-Pardo, O.; Fischer, M.; Gerschütz, F.; Koeth, J.; Krestnikov, I.; Kovsh, A.; Le Gouezigou, O. & Make, D., Uncooled Directly Modulated Quantum Dot Laser 10Gb/s Transmission at 1.3µm, with Constant Operation Parameters, European Conference on Optical Communication, Th 4.5.7, 2006.

Deppe, D.G.; Huang, H. & Shchekin, O.B., Modulation characteristics of quantum-dot lasers: the influence of p-type doping and the electronic density of states on obtaining high speed, *IEEE J. Quantum Electronics*, Vol. 38, 1587-1593, 2002.

Deubert, S.; Somers, A.; Kaiser, W.; Schwertberger, R.; Reithmaier, J.P. & Forchel, A., InP-based quantum dash lasers for wide gain bandwidth applications, *J. Cryst. Growth*, Vol. 278, 346-350, 2005.

Erneux, T.; Kovanis, V.; Gavrielides, A. & Alsing, P.M., Mechanism for period-doubling bifurcation in a semiconductor laser subject to optical injection , *Phys. Rev. A*, Vol. 53, 4372-4380, 1996.

Erneux, T.; Viktorov, E.A.; Mandel, P.; Azouigui, S. And Ramdane A., Relaxation characteristics of quantum-dash-based semiconductor lasers, Appl. Phys. Lett. 95, 231107, 2009

Fernier, B.; Adams, K.; Artigue, C.; Barrou, T.; Göth, A.; Grard, E.; Jörg, W.; Keller, D.; Lafragette, J.L.; Lestra, A.; Pagnod, P.; Rabaron, S.; Rainsant, J.M.; Scherb, J.; Toullier, D.; Tregoat, D. & and Rehm, W., 1.3 µm low cost plastic module for 622Mbit/s transmission at 85°C, in Proc. ECOC'98, Vol. 1, 445-446, 1998.

Franke, D.; Harde, P.; Boettcher, J.; Moehrle, M.; Sigmund, A. & Kuenzel, H., Improved emission wavelength reproducibility of InP-based all MOVPE grown 1.55 µm quantum dot lasers, International Conference on Indium Phosphide and Related Materials, FrB1.4, 2007.

Gerschütz, F.; Fischer, M.; Koeth, J.; Chacinski, M.; Schatz, R.; Kjebon, O.; Kovsh, A.; Krestinkov, I. & Forchel, A., Temperature insensitive 1.3-µm InGaAs/GaAs quantum dot distributed feedback lasers for 10Gbit/s transmission over 21 km, *Electron. Lett.*, Vol. 42, 1457-1458, 2006.

Grillot, F.; Thedrez, B.; Py, J.; Gauthier-Lafaye, O.; Voiriot, V. & Lafragette, J.L., 2.5 Gbit/s transmission characteristics of 1.3µm DFB lasers with external optical feedback, *IEEE Photon. Technol. Lett*, Vol. 14, 101-103, 2002.

Grillot, F.; Thedrez, B.; Voiriot, V. & Lafragette, J.L., Coherence collapse threshold of 1.3-µm semiconductor DFB lasers, *IEEE Photon. Technol. Lett.*, Vol. 1, 1-3, 2003.

[a]Grillot, F. ; Naderi, N.A. ; Pochet, M. ; Lin, C.-Y. & Lester, L.F., Variation of the Feedback Sensitivity in a 1.55µm InAs/InP Quantum-Dash Fabry-Perot Semiconductor Laser, *Appl. Phys. Lett.*, 13, 191108, 2008.

[b]Grillot, F. ; Dagens, B. ; Provost, J.G. ; Su, H. & Lester, L.F., Gain compression and above-threshold linewidth enhancement factor in 1.3-µm InAs/GaAs quantum dot lasers, *IEEE J. Quantum Electron.*, Vol. 44, 10, 946-951, 2008.

[c]Grillot, F.; Martinez, A.; Merghem. K.; Provost, J.G.; Alexandre, F.; Piron, R.; Dehaese, O.; Loualiche, S.; Lester, L.F. & Ramdane, A., Stable above-threshold linewidth enhancement factor in a 1.52-µm InAs/InP (311B) quantum dot laser, The 21st Annual Meeting of the IEEE LEOS, 535 – 536, 2008.

Gupta, J.A.; Barrios, P.J.; Caballero, J.A.; Poitras, D.; Aers, G.C.; Pakulski, G. & Wu, X., Gain and lifetime of GaInNAsSb narrow ridge waveguide laser diodes in continuous-wave operation at 1.56-µm, *Appl. Phys. Lett*, Vol. 89, 151119, 2006.

Helms, J. & and Petermann, K., Microwave modulation of semiconductor lasers with optical feedback, *Electron. Lett*., 25, 1369-1371, 1989.

Helms, J. & Petermann, K., A simple analytic expression for the stable operation range of laser diodes with optical feedback, *IEEE J. Quantum Electron*., Vol. 26, 833-836, 1990.

Henry, C.H., Theory of the linewidth of semiconductor lasers, *IEEE J. Quantum Electron*., 18, 259-264, 1982.

Henry, C.H. & Kazarinov, R.F., Instabilities of semiconductor lasers due to optical feedback from distant reflectors, *IEEE J. Quantum Electron*., Vol. 22, 294-301, 1986.

Hirota, O. & Suematsu, Y., Noise properties of injection lasers due to reflected waves, *IEEE J. of Quantum Electron*.,15, 142-149, 1979.

D. M. Kane and K. A. Shore, Unlocking dynamical diversity, Wiley, 2005.

Karachinsky, L.Ya.; Kettler, T.; Gordeev, N.Yu.; Novikov, I.I.; Maximov, M.V.; Shernyakov, Yu.M.; Kryzhanovskaya, N.V.; Zhukov, A.E.; Semenova, E.S.; Vasil'ev, A.P.; Ustinov, V.M.; Ledentsov, N.N.; Kovsh, A.R.; Shchukin, V.A.; Mikhrin, S.S.; Lochmann, A.; Schulz, O.; Reissmann, L. & Bimberg, D., High-power singlemode CW operation of 1.5 lm-range quantum dot GaAs-based laser, *Electron. Lett*., Vol. 41, 8-9, 2005.

Kim, J.S.; Lee, J.H.; Hong, S.U.; Han, W.S.; Kwack, H.; Lee, C.W. & OH, D.K., Room-temperature operation of InP-based InAs quantum dot laser, *IEEE Photon. Technol. Lett*, Vol. 16, 1607-1609, 2004.

Kitaoka, Y.; Sato, H.; Mizuuchi, K.; Yamamoto, K. & Kato, M., Intensity noise of laser diode with optical feedback, *IEEE J. of Quantum Electron.*, Vol. 32, 822-828, 1996.

Lang, R. & Kobayashi, K., External optical feedback effects on semiconductor injection laser properties, *IEEE J. Quantum Electron*., Vol. QE-16, 347-355, 1980.

Lelarge, F.; Dagens, B.; Renaudier, J.; Brenot, R.; Accard, A.; Van Dijk, F.; Make, D.; Le Gouezigou, O.; Provost, J.G.; Poingt, F.; Landreau, J.; Drisse, O.; Derouin, E.; Rousseau, B.; Pommereau, F. & Duan, G.H., Recent Advances on InAs/InP Quantum Dash Based Semiconductor Lasers and Optical Amplifiers Operating at 1.55-µm, *IEEE J. of Selected Topics in Quantum Electronics.*, Vol. 13, 111-124, 2007.

Lenstra, D.; Verbeek, B.H. & Den Boef, A.J., Coherence collapse in single-mode semiconductor lasers due to optical feedback, *IEEE J. Quantum Electron*., Vol. QE-21, 674-679, 1985.

Li, Y.; Naderi, N.A. ; Kovanis, V. & Lester, L.F., Modulation Response of an Injection-Locked 1550 nm Quantum Dash Semiconductor Laser, The 20th Annual Meeting of the IEEE LEOS, 498-499, 2007.

Liu, G.T.; Stintz, A.; Li, H.; Malloy, K.J. & Lester, L.F., Extremely low room-temperature threshold current density diode lasers using InAs dots in $In_{0.15}Ga_{0.85}As$ quantum well, *Electron. Lett*., Vol. 35, 1163-1165, 1999.

Liu, G.; Jin, X. & Chuang, S.L., Measurement of linewidth enhancement factor of semiconductor lasers using an injection-locking technique, *IEEE Photon. Technol. Lett*., Vol.13, 430 – 432, 2001.

Makino, S.; Shinoda, K.; Kitatani, T.; Tsuchiya, T. & Aoki, M., Wide temperature range (0 to 85°C), 40-km SMF transmission of a 1.55 μm, 10-Gbit/s InGaAlAs electroabsorption modulator integrated DFB laser, Technical Digest OFC, Vol. 6, 6-11, postdealine paper PDP14, 2005.

Martinez, A.; Lemaître, A.; Merghem, K.; Ferlazzo, L.; Dupuis, C.; Ramdane, A.; Provost, J.G.; Dagens, B.; Le Gouezigou, O. & Gauthier-Lafaye, O., Static and dynamic measurements of the α-factor of five-quantum-dot-layer single-mode lasers emitting at 1.3-μm on GaAs, *Appl. Phys. Lett*, Vol. 86, 211115, 2005.

Martinez, A.; Merghem, K.; Bouchoule, S.; Moreau, G.; Ramdane, A.; Provost, J.-G.; Alexandre, F.; Grillot, F.; Dehaese, O.; Piron, R. & Loualiche, S., Dynamic properties of InAs/InP(311B) quantum dot Fabry-Perot lasers emitting at 1.52-μm, *Appl. Phys. Lett*., Vol. 93, 021101, 2008.

Mi, Z.; Bhattacharya, P. & Yang, J., Growth and characteristics of ultralow threshold 1.45 m metamorphic InAs tunnel injection quantum dot lasers on GaAs, *Appl. Phys. Lett*., Vol. 89, 153109, 2006.

Mork, J.; Tromborg, B. & Mark, J., Chaos in semiconductor lasers with optical feedback: theory and experiment, *IEEE J. Quantum Electron*., Vol. QE-28, 11, 93-108, 1992.

Mork, J.; Tromborg, B. & Christiansen, P.L., Bistability and low-frequency fluctuations in semiconductor lasers with optical feedback: a theoretical analysis, *IEEE J. Quantum Electron*. Vol. 24, 123-133, 1988.

O'Brien, D.; Hegarty, S.P.; Huyet, G.; McInerney, J.G. ; Kettler, T.; Laemmlin, M. ; Bimberg, D.; Ustinov, V.M.; Zhukov, A.E. ; Sikhrin, S.S. & Kovsh, A.R., Feedback sensitivity of 1.3μm InAs/GaAs quantum dot lasers, *Electron. Lett*., 39, 1819-1820, 2003.

Petermann, K., Laser Diode Modulation and Noise, Kluwer Academic Publishers, 1988.

Petermann, K., External Optical Feedback Phenomena in Semiconductor Lasers, *IEEE J. of Select. Topics in Quantum Electronics*, Vol. 1, 480-489, 1995.

Phillips, A.F.; Sweeney, S.J.; Adams, A.R. & Thijs, P.J.A., Temperature dependence of 1.3- and 1.5-μm compressively strained InGaAs(P) MQW semiconductors lasers, *IEEE J. of Select. Topics in Quantum Electronics*, Vol. 5, 401-412, 1999.

Saito, H.; Nishi, K.; Kamei, A. & Sugou, S., Low chirp observed in directly quantum dot lasers, *IEEE Photon. Technol. Lett*, Vol. 12, 1298-1300, 2000.

Saito, H.; Nishi, K. & S. Sugou, Low chirp operation in 1.6-μm quantum dot laser under 2.5GHz direct modulation, *Electron. Letts*., 37, 1293-1295, 2001.

Shunk, N. & Petermann, K., Numerical analysis of the feedback regimes for a single-mode semiconductor laser with external feedback, *IEEE J. Quantum Electron*., Vol. 24, 1242-1247, 1988.

Shunk, N. & Petermann, K., Stability analysis for laser diodes with short external cavities, *IEEE Photon. Technol. Lett*., Vol.1, 49-51, 1989.

Sorin, W. V.; Chang, K. W.; Conrad, G. A. & Hernday, P. R., Frequency domain analysis of an optical FM discriminator, *J. Lightwave Technol*., Vol. 10, 787–793, 1992.

Stegmuller, B.; Borchert, B. & Gessner, R., 1.57-μm Strained-Layer Quantum-Well GaInAlAs Ridge-Waveguide Laser Diodes with High Temperature (130°C) and Ultrahigh-speed (17 GHz) Performance, *IEEE Photon. Technol. Lett*., Vol. 5, 597-599, 1993.

Su, H.; Zhang, L.; Gray, A.L.; Wang, R.; Newell, T.C.; Malloy, K.J. & and Lester, L.F., High external feedback resistance of laterally loss-coupled distributed feedback quantum dot semiconductor lasers, *IEEE Photon. Technol. Lett*., Vol.15, 1504-1506, 2003.

Su, H.; Zhang, L.; Gray, A.L.; Wang, R.; Newell, T.C.; Malloy, K.J. & Lester, L.F., Linewidth Study of InAs-InGaAs quantum dot distributed feedback lasers, *IEEE Photon. Technol. Lett.*, Vol.16, 2206-2208, 2004.

Su, H.; Zhang, L.; Gray, A.L.; Wang, R.; Varangis, P.M. & Lester, L.F., Gain compression coefficient and above-threshold linewidth enhancement factor in InAs/GaAs quantum dot DFB lasers, *Proceeding SPIE* 5722-11, 2005.

Su, H. & and Lester, L.F., Dynamic properties of quantum dot distributed feedback lasers: high speed linewidth and chirp, *J. Phys. D: Appl. Phys.*, Vol. 38, 2005.

Suhara, M. & and Yamada, M., Analysis of excess noise due to external optical feedback in DFB semiconductor lasers on the basis of the mode competition theory, *IEICE Trans. Electron.*, Vol. EC76-C, 6, 1007-1017, 1993.

Thijs, P. J. A; Tiemeijer, L.F.; Binsma, J.J.M & and Van Dongen, T., Progress in longwavelength strained-layer InGaAs(P) quantum-well semiconductor lasers and amplifiers, *IEEE J. Quantum Electron.*, Vol. 30, 477–499, 1994.

Tkach, R.W. & Chraplyvy, A.R., Regimes of feedback effects in 1.5-μm distributed feedback lasers, *J. Lightwave. Tech.*, Vol. LT-4, 1655-1661, 1986.

Tohmori, Y.; Itaya, Y. & Toba, H., 1.3 μm spot-size converter integrated laser diodes (SS-LDs) for access network applications, The 10th Annual Meeting of the IEEE LEOS, TuQ1, 270-271,1997.

Tromborg, B. & Mork, J., Non-linear injection locking dynamics and the onset of coherence collapse in external cavity lasers, *IEEE J. Quantum Electron.*, Vol. 26, 642-654, 1990.

Veselinov, K; Grillot, F.; Cornet, C.; Even, J.; Bekiarski, A.; Gioannini, M. & Loualiche, S., Analysis of the Double Laser Emission Occurring in 1.55μm InAs/InP (113)B Quantum-Dot Lasers, *IEEE J. Quantum Electron*, Vol. 43, 810-816, 2007.

Wang, R.H.; Stintz, A.; Varangis, P.M.; Newell, T.C.; Li, H.; Malloy, K.J. & Lester, L.F., Room-temperature operation of InAs quantum-dash lasers on InP (100), *IEEE Photon. Technol. Lett.*, Vol. 13, 767-769, 2001.

Wei, J. H. & Chan, K. S., A theoretical analysis of quantum dash structures, *J. Applied Phys.*, 97, 123524, 2005.

Yamada, M. & Suhara, M., Analysis of excess noise due to external optical feedback in semiconductor lasers on mode competition theory, *IEICE Trans. Electron.*, Vol. EC73-C, 77-82, 1990.

Acknowledgments

Authors are grateful to Professor Jean-Claude Simon, Head of FOTON for the financial support as well as for fruitful discussions. Authors acknowledge Professor Thomas Erneux from Brussels University and Professor Vassilios Kovanis from the US Air Force for fruitful discussions.

This work was supported in part by the Air Force Research Laboratory. The views expressed in this book chapter are those of the authors and do not reflect the official policy or positions of the United States Air Force, Department of Defense, or the US government.

IntechOpen

Semiconductor Technologies

Edited by Jan Grym

ISBN 978-953-307-080-3
Hard cover, 462 pages
Publisher InTech
Published online 01, April, 2010
Published in print edition April, 2010

Semiconductor technologies continue to evolve and amaze us. New materials, new structures, new manufacturing tools, and new advancements in modelling and simulation form a breeding ground for novel high performance electronic and photonic devices. This book covers all aspects of semiconductor technology concerning materials, technological processes, and devices, including their modelling, design, integration, and manufacturing.

How to reference

In order to correctly reference this scholarly work, feel free to copy and paste the following:

F. Grillot, N. A. Naderi, M. Pochet, C.-Y. Lin and L. F. Lester (2010). The Critical Feedback Level in Nanostructure - Based Semiconductor Lasers, Semiconductor Technologies, Jan Grym (Ed.), ISBN: 978-953-307-080-3, InTech, Available from: http://www.intechopen.com/books/semiconductor-technologies/the-critical-feedback-level-in-nanostructure-based-semiconductor-lasers

INTECH
open science | open minds

InTech Europe
University Campus STeP Ri
Slavka Krautzeka 83/A
51000 Rijeka, Croatia
Phone: +385 (51) 770 447
Fax: +385 (51) 686 166
www.intechopen.com

InTech China
Unit 405, Office Block, Hotel Equatorial Shanghai
No.65, Yan An Road (West), Shanghai, 200040, China
中国上海市延安西路65号上海国际贵都大饭店办公楼405单元
Phone: +86-21-62489820
Fax: +86-21-62489821

IntechOpen